Received August 21, 2014, accepted October 20, 2014, date of publication October 23, 2014, date of current version November 5, 2014.

Digital Object Identifier 10.1109/ACCESS.2014.2364638

A 15-Gb/s Wireless ON-OFF Keying Link

LARS OHLSSON AND LARS-ERIK WERNERSSON
Department of Electrical and Information Technology, Lund University, Lund 22100, Sweden
Corresponding author: L. Ohlsson (lars.ohlsson@eit.lth.se).

This work was supported in part by the Swedish Foundation for Strategic Research, in part by the Swedish Research Council, and in part by the Knut and Alice Wallenberg Foundation.

ABSTRACT Bit-error rate measurements for ON-OFF keying modulation at multigigabit per second rates over a V-band wireless link are presented. Serial data-rates from 2.5 to 20 Gb/s were studied for a 2^{31}-1 bit random sequence. Error-free data transfer over a 0.3-m link was achieved at up to 10 Gb/s. Acceptable bit-error rates, $<10^{-5}$ and 10^{-3}, were measured at up to 1.5 m for 10- and 15-Gb/s data-rate, respectively. The performance was achieved using a transmitter that consists of an integrated wavelet generator, whereas the receiver was built from off-the-shelf waveguide components. The results demonstrate that very high data-rates may be achieved using binary modulation and short symbols generated in an efficient V-band transmitter. The system is benchmarked against state-of-the-art transceiver systems with multigigabit per second data-rates.

INDEX TERMS Multi-Gb/s, on-off keying (OOK), wireless communication.

I. INTRODUCTION

Wireless communication at data-rates exceeding 100 Gb/s are required to meet future demands [1]. Long-haul fibre links already show performance in excess of this [2], and last-mile millimetre-wave links are considered for wireless back-haul between cellular access points [3]. As of today, the standards for short-range multi-Gb/s wireless access, e.g. IEEE 802.15.3c, specify operation over up to 10 m at data-rates of a few Gb/s [4]. However, there are application areas which require even higher data-rates over shorter distances. One example is the computation area, where chip-to-chip communication and intra-connects can provide reduced routing complexity [5], [6]. Another example is wireless personal area networks (WPANs), where indoors streaming of media, kiosk downloads, and rapid device synchronisation is attractive [7], [8]. To achieve the required performance in such wireless systems, the limits of data-rate, energy-efficiency, and range in Gb/s wireless links must be investigated outside the present frameworks of standardisation. Such implementations may be operated in un-licensed bands, and pave the road towards future standardisation.

Interestingly, the targeted digital modulation format affects the front-end design challenges. To illustrate this, symbol sequences of typical modulation schemes are exemplified in Fig. 1. On the one hand, binary amplitude-shift keying (2-ASK) allows each radio symbol to hold one bit of data. A high data-rate thereby implies an equally high symbol-rate. This is the case for on-off keying (OOK), as illustrated in Fig. 1(a), which is a popular full-level 2-ASK sub-format.

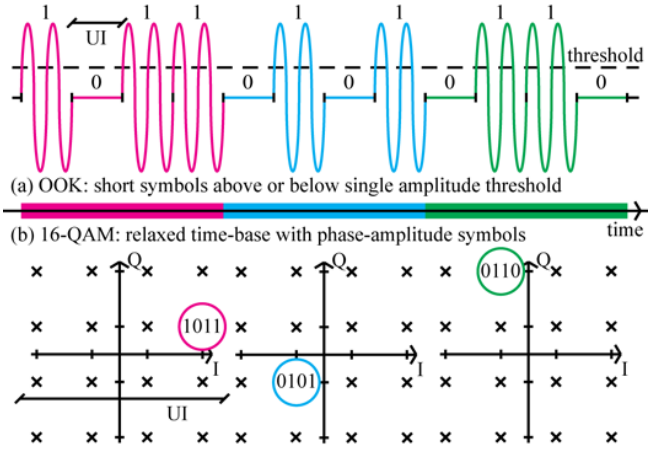

FIGURE 1. Illustration of two typical modulation schemes which can provide wireless Gb/s performance between integrated front-ends. (a) OOK is based on rapid switching about a threshold level, while (b) 16-QAM relies on accurately defined and detected phase-amplitude changes in the signal.

In OOK, the transmitter turns the carrier signal on and off and the receiver evaluates if the signal exceeds a certain threshold level. Wavelet generators and fast energy detection receivers [9], [10], may be used to push the performance in such spread-spectrum systems by increased symbol-rate. On the other hand, for high-order modulation schemes, a quantised constellation of unique phase-amplitude symbols maps the permutations of a multi-bit sequence. This is utilised, e.g. in 4-bit quadrature amplitude

modulation (16-QAM), as shown in Fig. 1(b). To achieve a certain data-rate, the QAM symbol-rate can be relaxed by a factor equal to the number of bits per symbol. The symbol unit interval (UI), as illustrated in Fig. 1, is thereby prolonged and more time may be spent on hardware processing, e.g. sampling in analogue-to-digital converters. However, signal mixing, amplification, and sampling in high-order modulation schemes results in increased power dissipation. The increase is typically a factor of 10 in the transmitter and a factor of 5 in the receiver, based on current multi-Gb/s implementations [11], [12], which may be significant in battery-powered applications. The QAM sub-format of quadrature phase-shift keying (QPSK) has the property of constant power-level in all symbols. This ideally means that the dynamic range of the receiver may be reduced. However, to combat the influences of path-loss variation in the wireless link, e.g. from changing distance and signal fading, high receiver dynamic range, e.g. via baseband limiting amplifiers [13], is beneficial for all the above modulations.

To realise better transceivers, device optimisation and circuit innovation in silicon and various III-V technologies continues to be explored extensively in the millimetre-wave spectrum, 30–300 GHz, [14]. On the one hand, implementations in silicon technology allows for digital signal processing in complementary logic at a high integration level. This alleviates the implementation of I/O buffers, high-order modulation schemes [15], and hybrid switching transmitters [16]. On the other hand, III-V technologies provide advanced devices and improved transistor performance, especially with the recent development of III-V metal-oxide-semiconductor field-effect-transistors (MOSFETs). Specifically, III-V MOSFETs currently provide high transconductance and low on-resistance, as compared to other III-V transistors [17], and can be used as rapid switches [9]. Such transistors may be exploited in high-speed short-range wireless communication where efficient and simplistic implementations need to be considered to maintain energy-efficiency. Further, resonant-tunneling diodes (RTDs) in III-V heterostructures may be used for signal generation up to the THz-spectrum [18]. Schottky diodes, or heterojunction backward diodes [19], may be used in envelope detectors, providing down-conversion of multi-Gb/s OOK signals [20]. Systems in III-V technology also have access to low-loss passives and efficient antennas on-chip based on the insulating substrate [21]. Ultimately, to access wider channel bandwidths that allow higher symbol-rates, a shift towards front-end technologies operating at higher frequencies, will be required. Also, scaling towards terahertz frequencies makes it feasible to reduce the physical size of antenna elements and arrays [22].

In this paper, we demonstrate wireless communication measurements at serial data-rates up to 20 Gb/s. A III-V wavelet generator with sub-period start-up [9] is used together with off-the-shelf V-band, 50–75 GHz, components in waveguide assemblies. We also evaluate and discuss the transmitter and receiver performance, including output power, sensitivity, and energy-efficiency. Also, the concept of transceiver omni-distance is defined and utilised for benchmarking.

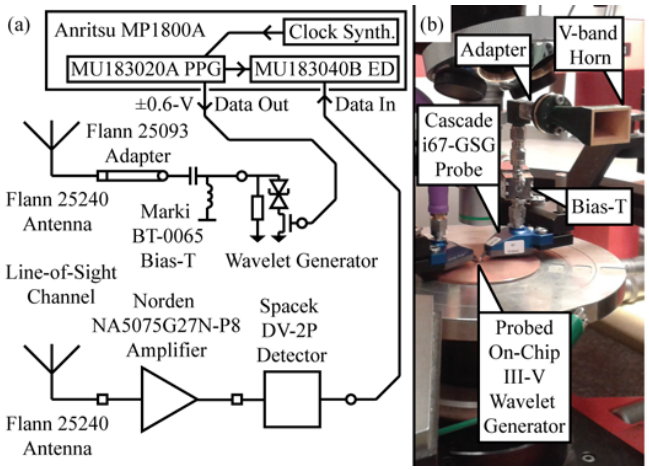

FIGURE 2. Transceiver for Gb/s on-off keying communication. (a) Schematic setup for bit-error rate measurements, and (b) photograph of transmitter.

II. MULTI-Gb/s WIRELESS TRANSCEIVERS

In recent years, the first wireless transceiver front-ends operating at data-rates approaching, or exceeding, 10 Gb/s have been demonstrated. Most of these multi-Gb/s implementations operate in the V-band. Transmitter front-ends typically achieve output power levels ranging from 0 to +10 dBm, and have been implemented for OOK [11], [13], [23]–[25], 2-ASK [5], [6], [10], [26], QPSK [15], [27]–[29], and 16-QAM [12], [15], [30], [31]. Receiver front-ends for ASK and OOK operate by energy detection to demodulate the data, with demonstrated input referred sensitivities as low as –33.7 dBm [10]. For demodulation of phase-defined symbols, e.g. 4-QPSK and 16-QAM, coherent receivers are required. QAM receiver front-ends have been shown with sensitivity levels of –54.2 dBm, but their symbol-rates are currently limited to about 4 GS/s [12]. Finally, wireless communication between multi-Gb/s transceivers has also been demonstrated. The record link distance of 3 m was achieved for 2-ASK at a bit-rate of 12 Gb/s using high-gain horn antennas [10]. By use of integrated antennas separated by a 5 mm link, a data-rate of 10 Gb/s/channel was achieved in two parallel 2-ASK streams diplexed in 57 and 80 GHz channels [6]. However, by use of integrated antennas communicating in 16-QAM over 20 cm, a data-rate of 16 Git/s has been demonstrated [12].

To allow a comparison of wireless transceivers in various implementations, a set of applicable figures-of-merit needs to be defined. The link budget in line-of-sight is set by the transmitter output power, P_{Tx}, the receiver sensitivity, S, i.e. minimum received input power, P_{Rx}, which can be detected, via Frii's transmission equation

$$P_{\mathrm{Rx}} = P_{\mathrm{Tx}} G_{\mathrm{A,Tx}} \left(4\pi d f_{\mathrm{c}}/c\right)^2 G_{\mathrm{A,Rx}}/L \,, \qquad (1)$$

IEEE Access
The journal for rapid open access publishing

where $G_{A,Tx}$ and $G_{A,Rx}$ are the realised gains of the transmit and receive antennas, respectively, d is the link distance, f_c is the carrier frequency, L is the implementation loss, and c is the speed of light. The transmit and receive antennas are often equal, allowing a more compact notation for their gain, $G_A = G_{A,Tx} = G_{A,Rx}$. The power dissipations of the transmitter, $P_{dc,Tx}$, and receiver, $P_{dc,Rx}$, front-ends are intuitively found from the products of bias current and voltage. The total power dissipation of the transceiver, $P_{dc} = P_{dc,Tx} + P_{dc,Rx}$, when operated at a certain bit-rate, r, may be used to define the transceiver energy-efficiency, $EE = P_{dc}/r$. Further, having evaluated the link for a random symbol sequence at the limit of an acceptable bit-error probability, p_e, the normalised transceiver energy-efficiency, $NEE = P_{dc}/(rd)$, is found.

Portable wireless multi-Gb/s transceivers must be able to achieve a certain link distance by the use of integrated antennas, but front-ends are often evaluated using external antennas. To allow a comparison of transceiver front-end pairs tested under various conditions, the antenna gain and achieved link distance may be used to evaluate the equivalent omni-distance, or intrinsic front-end distance, d_i. The omni-distance is defined here as the equivalent link distance when using hypothetical omni-directional antennas with unit radiation efficiency. This is a representative figure-of-merit for comparison of the intrinsic performance of front-end transceivers, although antenna distortion is a variable of uncertainty if the antenna technologies differ significantly. A rigorous definition of the omni-distance was derived by use (1), equating the transmission loss for the implemented antenna gains and the link distance to the corresponding expression for $G_A = 0$-dBi antennas at the omni-distance. Consequently, it is found that

$$d_i = d/\sqrt{G_{A,Tx}G_{A,Rx}} \cong d/G_A, \qquad (2)$$

where the final approximation assumes equal transmit and receive antennas. Given knowledge of the transceiver omni-distance, it follows from (1) that the achievable link distance is doubled for every 6 dB of added transmission gain. Further, an omni-transceiver energy-efficiency, $NEE_i = P_{dc}/(rd_i)$, is also defined. This figure-of-merit is used to evaluate the normalised transceiver energy-efficiency without influence of the specific antenna gain in the test setup.

In chip-to-chip scenarios, typical link distances of 10 mm and compact antennas with 0 dBi gain, i.e. dipole- or patch-like directivity and a few decibels of radiation loss, can be assumed [5]. Corresponding specifications for WPAN scenarios are link distances of at least 50 mm and, as larger areas may be populated on- or off-chip, antenna gains of approximately 7 dB [11]. In both of the above cases, this results in a required omni-distance of $d_i = 10$ mm for short-range multi-Gb/s wireless transceiver front-ends.

III. OOK TRANSCEIVER SETUP

To test the limits of OOK modulation, a transceiver was implemented as illustrated in Fig. 2(a). An Anritsu MP1800A Signal Quality Analyzer, equipped with a 32-Gb/s pulse pattern generator (PPG) and a high-sensitivity error detector (ED), was used to generate data patterns and evaluate received errors. No clock-recovery was implemented and the clock was instead wired directly from the PPG to the ED. An $n = 2^N - 1 = 2^{31} - 1$ bit pseudo-random binary sequence (31-PRBS) of data with high and low levels of $+0.6$ and -0.6 V, respectively, was fed to the probed V-band transmitter front-end. As applicable for OOK, the data-sequence was translated into carrier on- and off-states for high and low level, respectively.

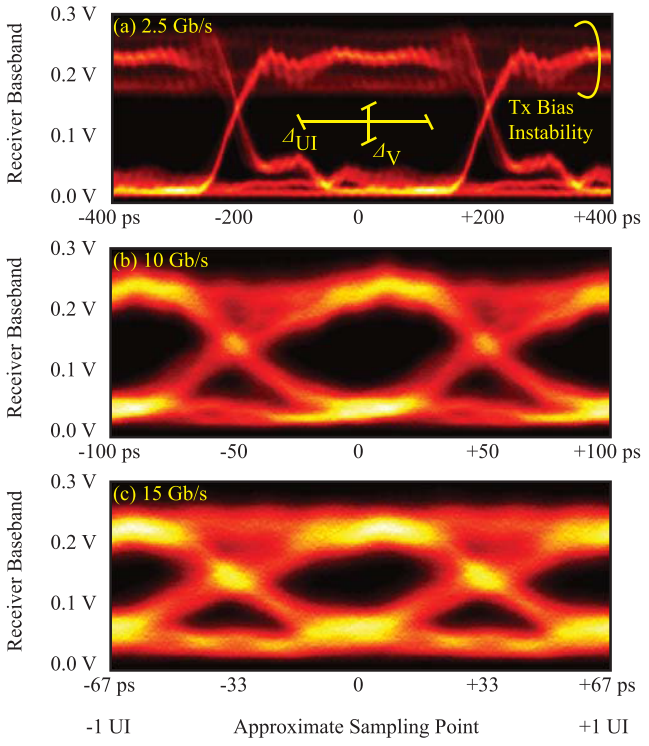

FIGURE 3. Measured symbol eye diagrams for a 15-PRBS at 0.3-m channel distance. The data-rate is (a) 2.5, (b) 10, and (c) 15 Gb/s. A schematic illustration of the eye margins is shown on the 2.5-Gb/s eye.

A coherent RTD-MOSFET wavelet generator with sub-period start-up and quench was used to up-convert the input baseband data-pattern to the V-band. Using the same device design but a more streamlined processing scheme, this wavelet generator was based on a previous implementation [9]. It provided an output power level of approximately $+5$ dBm at 62.5-GHz carrier-frequency in the on-state. In the off-state, the 130-nm III-V MOSFET implemented in series with the 35-μm^2 RTD blocked the bias current and no oscillation was generated. The output of the wavelet generator was probed with an RF-probe and the signal was then fed to a 20-dBi gain V-band horn antenna via a bias-T and an adapter, as shown in Fig. 2(b). The probe, bias-T, and adapter have insertion loss specifications of 1 dB, 2 dB, and 1 dB, respectively, corresponding to implementation loss of approximately $L = 4$ dB. The signal was sent over a line-of-sight channel at link distances of $d =$

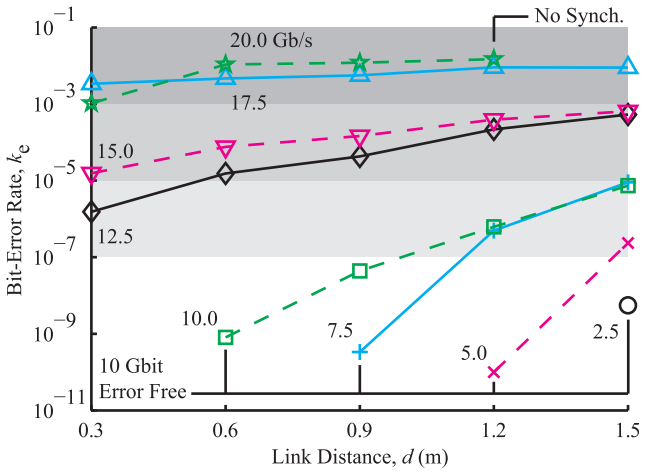

FIGURE 4. Measured wireless 2.5 to 20-Gb/s on-off keying bit-error rate in a line-of-sight scenario. The carrier-frequency was approximately 62.5 GHz.

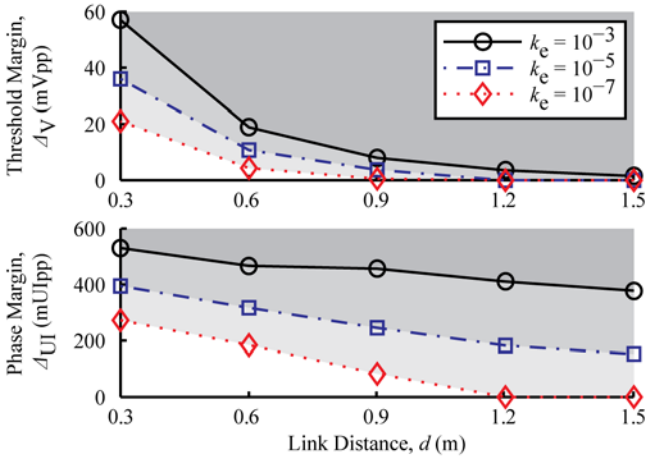

FIGURE 5. Measured eye margins for bit-error rates $k_e < 10^{-3}$, 10^{-5}, and 10^{-7} at 10 Gb/s data-rate, i.e. with a 100-ps UI. Both margins, i.e. threshold, Δ_V, and phase, Δ_{UI}, are given peak-to-peak at the sampling point.

0.3, 0.6, 0.9, 1.2 and 1.5 m. In such far-field line-of-sight, the channel pathloss, L_{FS}, may be identified from (1) as $L_{FS} = (4\pi df_c/c)^2$. The pathloss levels at the realised link distances were thereby varied from 57.9 dB to 71.8 dB. Further, the evaluated link distances correspond to omni-distances up to 15 mm.

On the receiving side, an identical horn antenna was connected directly to the waveguide input of a V-band amplifier. This amplifier provided nominally 26 dB gain from 50 to 75 GHz, and consumed 243 mA at 12 V bias. The total receiver power dissipation was thereby 2.92 W. The amplified waveform was de-modulated using a V-band envelope detector, converting its input power to a received baseband voltage. This zero-bias detector has a mean specified continuous-wave voltage sensitivity of 2.9 V/mW at –20-dBm input level for 1-MΩ termination of the IF-output. In the setup used here, however, the non-linear detector was terminated with the 50-Ω input of the ED. This drastically lowered the detector voltage sensitivity, but also reduced its symbol transition-time, i.e. widening its IF-bandwidth for high-rate operation. The resulting input referred receiver sensitivity level is evaluated below.

In the MP1800A, the received energy detector output signal was synchronised to find the ideal sampling point within the symbol UI. A total of number of $m = 10^{10}$ bits, i.e. 10 Gbits in binary OOK, were evaluated for each measurement. The number of received faulty bits, m_e, was used to calculate the ratio of erroneous bits, $k_e = m_e/m$, commonly and ambiguously referred to as bit-error rate. This is a good estimate of the bit-error probability, $p_e \approx k_e$, if the utilised PRBS is long enough to emulate a random sequence when repeated. It has been shown for similar systems that bit-error rate results may be strongly underestimated if the utilised PRBS length is too short to provide appropriate randomness [13]. Eye diagrams were captured using a LeCroy 100H oscilloscope with a SE-100 sampling head connected to the receiver output, for a 15-PRBS of data due to post-processing memory limitations.

IV. OOK TRANSCEIVER RESULTS

The RTD-MOSFET was biased at 1.85 V and consumed up to 13.5 mA, increasing with data-rate, yielding transmitter front-end energy-efficiencies, $EE_{Tx} = P_{dc,Tx}/r$, down to 1.25 pJ/bit. Specifically, the realised transmitter front-end energy-efficiencies were $EE_{Tx} = 7.70$, 4.00, 2.79, 2.17, 1.81, 1.55, 1.36, and 1.25 pJ/bit, respectively, for the data-rates increasing in equal steps from $r = 2.5$ to 20.0 Gb/s. This compares favourably to a state-of-the-art V-band transmitter implementation in silicon technology where the transmitter achieves 2.94 pJ/bit at 10.7 Gb/s [11]. The resulting receiver power dissipation, receiver front-end energy-efficiency, $EE_{Rx} = P_{dc,Rx}/r$, and the total transceiver energy-efficiency are high, as compared to state-of-the-art. In Table I, which will be discussed below, the summarised performance of the OOK transceiver is compared to state-of-the-art implementations for wireless multi-Gb/s communication systems.

The received symbol eye diagrams at 0.3 m channel distance, captured at 2.5, 10, and 15-Gb/s data-rate are shown in Fig. 3(a-c), respectively. Increasing the data-rate, the eye has a saturated region around the sampling-point up to approximately $r = 10$-Gb/s, as seen in Fig. 3(b), where the symbol UI is $1/r = 100$ ps. At this data-rate, the symbol transition-time is of approximately the same length as the UI. The eye thereby starts to close at higher data-rates, as can be seen in Fig. 3(c). From the link budget defined by (1), i.e. $P_{Rx} = P_{Tx}G_A^2/(L_{FS}L)$, the input power level to the receiver amplifier was found to range from –16.9 to –30.9 dBm as the channel distance was increased from 0.3 to 1.5 m, respectively. After amplification and conversion to baseband, the maximum detector amplitudes were 297 mV at the shortest distance, and 54 mV at the longest link distance. The received on-level is seen, in Fig. 3(a), to be distributed peculiarly at

IEEE Access
The journal for rapid open access publishing

TABLE 1. Benchmark comparison of multi-Gb/s wireless transceivers.

Quantity	*Symbol* (Unit)	[11]	[5]	[13]	[10]	[15] [a]	[12] [a]	This Work
Author Affiliations	——	K.A.I.S.T. (Daejeon)	Sony Corp. (Tokyo)	Southeast U. (Nanjing)/ E.P. Montreal	Hiroshima U. (Higashi-Hiroshima)	Tokyo I.T./ Sony Corp. (Tokyo)	Tokyo I.T.	Lund U.
Publication Year	——	2013	2010	2014	2013	2011	2011	2014
Circuit Technology	——	90-nm CMOS	40-nm CMOS	90-nm CMOS	40-nm CMOS	65-nm CMOS	65-nm CMOS	130-nm III-V
Antenna Technology	——	On-board Yagi-Uda	On-board Bond-Wire	On-board Yagi-Uda	D-band Horn	On-board Aperture	On-board Aperture	V-band Horn
Modulation Format	——	OOK	2-ASK	OOK	2-ASK	4-QPSK/ 16-QAM	16-QAM	OOK
Centre-Frequency	f_c (GHz)	60	57	45	134	60.5	60.5	62.5
Data-Rate	r (Gb/s)	10.7	11	5	12	8/ 11	**16**	10/ 15
Limit Bit-Error Rate	k_e (m_e/m)	10^{-12}	10^{-11}	10^{-12}	10^{-5}	10^{-3} [a]	10^{-3} [a]	10^{-5}/ 10^{-3}
PRBS Exponent	N	7	7	7	31	—— [a]	—— [a]	31
Transmitter Power-Dissipation	$P_{dc,Tx}$ (mW)	31.5	29	61.6	77.0	252	247	**21.6/ 23.3**
Transmitter Energy-Efficiency	EE_{Tx} (pJ/bit)	2.94	2.64	12.3	6.42	31.5/ 22.9	15.4	**2.17/ 1.55**
Output-Power [b]	P_{Tx} (dBm)	+4.4	0	+7.6	+2.8	**+9.5**	+5.4	+5
Receiver Power-Dissipation	$P_{dc,Rx}$ (mW)	**36.0**	41	53.6	132	172	204	2920
Receiver Energy-Efficiency	EE_{Rx} (pJ/bit)	**3.36**	3.73	10.7	11.0	21.6/ 15.6	12.8	292/ 194
Sensitivity [c]	S (dBm)	–30.4	–30.5	–32.5	–33.7	–28.6/ –38.1	**–54.2**	–30.9
Transceiver Power-Dissipation	P_{dc} (mW)	**67.5**	70	115	209	424	451	2940
Transceiver Energy-Efficiency	EE (pJ/bit)	**6.31**	6.36	23.0	17.4	53.0/ 38.5	28.2	294/ 196
Antenna Gain	G_A (dBi)	6.6	0	8.7	24	2	2	20
Link Distance	d (m)	0.10	0.014	0.40	**3.00**	0.05	0.20	1.50
Omni-Distance [d]	d_i (mm)	21.9	14.0	54.0	11.9	31.5	**126**	15.0
Normalised Transceiver Energy-Efficiency	NEE (pJ/bit/m)	63.1	455	57.6	**5.81**	1060/ 771	141	196/ 131
Omni-Transceiver Energy-Efficiency [e]	NEE_i (pJ/bit/mm)	0.288	0.455	0.427	15.8	1.68/ 1.22	**0.223**	19.6/ 13.1

The transceivers are ordered with increasing power dissipation from left to right. The three best implementations are highlighted by shading for figures-of-merit (rows) where "good" or "bad" is well-defined; the best is indicated by bold font.

[a] The high-order implementations have high limit bit-error rates at unknown PRBS lengths [12] [15], challenging the validity of the comparison.

[b] Output power is the high symbol power for OOK, 2-ASK, the constant symbol power for 4-QPSK, and the maximum symbol power for 16-QAM.

[c] Sensitivity is stated as the power at the receiver antenna port which must be detected during the benchmarked communication measurements, found via (1). This is the high symbol power for OOK and 2-ASK, the constant symbol power for 4-QPSK, and the minimum symbol power for 16-QAM. Assuming an even-spaced voltage constellation with equal probability for 16-QAM, the average symbol power is –2.55 dBmax and the minimum symbol power is –9.54 dBmax.

[d] Omni-distance is the link distance normalised over the antenna gain according to (2), for front-end comparison.

[e] Omni-transceiver energy-efficiency is the transceiver energy-efficiency normalised over the omni-distance, for front-end comparison.

2.5-Gb/s, as compared to the more Gaussian distributions seen at higher data-rates. This is attributed to transmitter bias instability when the on-state is held continuously, i.e. for several repeated 2.5-Gb/s on-symbols. Also, a noticeable level of detector RF-leakage can be seen as an approximately $1/f_c = 16$-ps ripple on the eye diagram.

Bit-error rate, k_e, measurements were performed at the five channel distances and the results are shown in Fig. 4. It is seen that more errors were captured for increasing data-rate and channel distance, as expected. It is especially noted that error-free transmission of a 10 Gbit data-sequence was achieved at data-rates up to 10 Gb/s over a 0.3-m channel. This corresponds to a normalised transceiver energy-efficiency of 1 nJ/bit/m. In a WPAN implementation, bit-error rates up to 10^{-5} or even 10^{-3} may be viable. This is visualised by increased levels of shading in Fig. 4 and Fig. 5. For these limit bit-error rates, data-rates up to 10 or 15-Gb/s, respectively, qualify as viable at 1.5 m link distance and the corresponding input referred sensitivity is –30.9 dBm. Interestingly, the bit-error rate results are seen to degrade significantly as the data-rate is increased from 10 to 12.5 Gb/s. We attribute this to the closing of the symbol eye, as seen in Fig. 3, where the symbol transition-time was identified to be 100-ps. Further, pattern synchronisation at 20 Gb/s was

only possible over link distances up to 1.2 m. To convey additional details of the link properties at 10-Gb/s data-rate, the measured eye margins, as indicated in Fig. 3(a), are shown in Fig. 5 for different limit values of bit-error rate. The phase margin, Δ_{UI}, has an approximately linear dependence on the channel distance, while the corresponding trend for the threshold margin, Δ_V, is seen to decay exponentially. This is attributed to the combination of link pathloss and detector non-linearity.

V. DISCUSSION

The III-V system presented in this paper has unique functionality, as compared to silicon implementations, what provides performance benefits. On the transmitter side, the RTD-MOSFET wavelet generator provides coherency and frequency scalability [9]. This allows for system design in the millimetre-wave spectrum, and scaling towards terahertz frequencies where spread-spectrum signals may be used in unlicensed bands [22]. On the receiving side, the zero-bias property of the detector allows for energy-efficient down-conversion. As an alternative to the utilised off-the-shelf power-hungry amplifier and bulky antennas, a more efficient and integrated amplifier and antenna implementation in III-V or silicon would improve the performance of the receiver. Receiver and antenna options can be found in the literature, as summarised below and benchmarked in Table I.

The here presented transceiver system, i.e. III-V wavelet generator, to amplifier, and zero-bias detector must be benchmarked against other implementations for short-range high-speed communication. For this purpose, state-of-the-art wireless multi-Gb/s transceivers have been summarised in Table I. The selection include all systems, to the best of our knowledge, which have demonstrated data-rates exceeding 3 Gb/s for omni-distances above 10 mm at disclosed PRBS lengths and limit bit-error rates. An exception on the disclosure of the PRBS length was made for the 4-QPSK and 16-QAM transceivers [12], [15], allowing a comparison across additional modulation formats. Certain transceiver implementations of significance did not fit within the selection criteria for this benchmark comparison. For example, transceiver chipsets implemented for 60 GHz communication within IEEE 802.11a have been shown [27], [28], [30]. Another, more recent, front-end implementation targets the IEEE 802.15.3c specification [31]. Spread-spectrum implementations such as 60-GHz OOK front-ends have also been shown [23]. Implementations with antennas in-package typically achieve data-rates of a few Gb/s [24], [25].

From Table I, it is clear that OOK and 2-ASK transceivers have lower power-dissipation than their multi-Gb/s QPSK or QAM counterparts. The most energy-efficient transceiver has achieved OOK communication at only 6.31 pJ/bit [11]. However, the RTD-MOSFET transmitter presented here has demonstrated the highest OOK data-rate and the best transmitter energy-efficiency in the comparison. The output power is competitive and the link distance is high, as compared to most other implementations. However, the link distances for all systems in Table I are seen to scale in proportion to the gain of the utilised antennas. The best omni-distance, i.e. intrinsic front-end distance without antenna gain, is achieved by the 16-QAM system using low-gain in-package antennas [12]. The 16-QAM implementation also has the best sensitivity, and achieves the highest data-rate. A general, and intuitive, observation is that the best performance in relation to invested energy, measured as a minimum in omni-transceiver energy-efficiency, is found for combinations of low power dissipation, high output power, and low sensitivity [11]–[13].

VI. CONCLUSION

Wireless OOK communication at up to, unprecedented, 20 Gb/s serial data-rates have been demonstrated. The utilised III-V transmitter front-end has high energy-efficiency and long link distances were achieved, as compared to state-of-the-art integrated multi-Gb/s transceivers. Viable performance was measured over channel distances up to 1.5 m at data-rates of 10 and 15 Gb/s for bit-error rate $k_e < 10^{-5}$ and 10^{-3}, respectively. The corresponding transmitter energy efficiencies are 2.17 and 1.55 pJ/bit. At 10 Gb/s data-rate, error-free transfer of 10 Gbit data in a 31-PRBS was possible over a 0.3 m link. The normalised transceiver energy-efficiency was 131 pJ/bit/m at 15 Gb/s data-rate over a 1.5 m line-of-sight channel; dominated to more than 99% by the receiver amplifier. The transceiver omni-distance was 15 mm, and the corresponding omni-transceiver energy-efficiency was hence 13.1 pJ/bit/mm. In the design of future spread-spectrum systems, III-V components allow for unique options in the transceiver architecture, regarding coherent signal generation, millimetre-wave frequency scaling, and energy-efficiency. This will improve the performance of portable, battery-powered, high-rate, and compact wireless links for short-range computation and WPAN applications.

ACKNOWLEDGMENT

The authors would like to thank J. Rasmussen and A. Messina, Anritsu, for providing the MP1800A system for the measurements campaign. The authors also thank J. B. Anderson, F. Tufvesson, and C. Gustafson, Lund University, for stimulating discussions.

REFERENCES

[1] P. Smulders, "The road to 100 Gb/s wireless and beyond: Basic issues and key directions," *IEEE Commun. Mag.*, vol. 51, no. 12, pp. 86–91, Dec. 2013.

[2] H. Bissessur *et al.*, "3.2 Tbit/s (80 × 40 Gbit/s) phase-shaped binary transmission over 3 × 100 km with 0.8 bit/s/Hz efficiency," *Electron. Lett.*, vol. 38, no. 8, pp. 377–379, Apr. 2002.

[3] S. Rangan, T. S. Rappaport, and E. Erkip, "Millimeter-wave cellular wireless networks: Potentials and challenges," *Proc. IEEE*, vol. 102, no. 3, pp. 366–385, Mar. 2014.

[4] T. Baykas *et al.*, "IEEE 802.15.3c: The first IEEE wireless standard for data rates over 1 Gb/s," *IEEE Commun. Mag.*, vol. 49, no. 7, pp. 114–121, Jul. 2011.

[5] K. Kawasaki *et al.*, "A millimeter-wave intra-connect solution," *IEEE J. Solid-State Circuits*, vol. 45, no. 12, pp. 2655–2666, Dec. 2010.

[6] Y. Tanaka *et al.*, "A versatile multi-modality serial link," in *IEEE Int. Conf. Solid-State Circuits Tech. Dig. Papers (ISSCC)*, Feb. 2012, pp. 332–334.

[7] R. C. Daniels, J. N. Murdock, T. S. Rappaport, and R. W. Heath, "60 GHz wireless: Up close and personal," *IEEE Microw. Mag.*, vol. 11, no. 7, pp. 44–50, Dec. 2010.
[8] C. Park and T. S. Rappaport, "Short-range wireless communications for next-generation networks: UWB, 60 GHz millimeter-wave WPAN, and ZigBee," *IEEE Trans. Wireless Commun.*, vol. 14, no. 4, pp. 70–78, Aug. 2007.
[9] M. Egard, M. Ärlelid, L. Ohlsson, B. M. Borg, E. Lind, and L.-E. Wernersson, "$In_{0.53}Ga_{0.47}As$ RTD–MOSFET millimeter-wave wavelet generator," *IEEE Electron Device Lett.*, vol. 33, no. 7, pp. 970–972, Jul. 2012.
[10] K. Katayama, M. Motoyoshi, K. Takano, L. C. Yang, and M. Fujishima, "209 mW 11 Gbps 130 GHz CMOS transceiver for indoor wireless communication," in *Proc. IEEE Asian Solid-State Circuits Conf. (A-SSCC)*, Nov. 2013, pp. 409–412.
[11] C. W. Byeon, C. H. Yoon, and C. S. Park, "A 67-mW 10.7-Gb/s 60-GHz OOK CMOS transceiver for short-range wireless communications," *IEEE Trans. Microw. Theory Techn.*, vol. 61, no. 9, pp. 3391–3401, Sep. 2013.
[12] H. Asada *et al.*, "A 60GHz 16Gb/s 16QAM low-power direct-conversion transceiver using capacitive cross-coupling neutralization in 65 nm CMOS," in *Proc. IEEE Asian Solid State Circuits Conf. (A-SSCC)*, Nov. 2011, pp. 373–376.
[13] F. Zhu *et al.*, "A low-power low-cost 45-GHz OOK transceiver system in 90-nm CMOS for multi-Gb/s transmission," *IEEE Trans. Microw. Theory Techn.*, vol. 62, no. 9, pp. 2105–2117, Sep. 2014.
[14] T. S. Rappaport, J. N. Murdock, and F. Gutierrez, "State of the art in 60-GHz integrated circuits and systems for wireless communications," *Proc. IEEE*, vol. 99, no. 8, pp. 1390–1436, Aug. 2011.
[15] K. Okada *et al.*, "A 60-GHz 16QAM/8PSK/QPSK/BPSK direct-conversion transceiver for IEEE802.15.3c," *IEEE J. Solid-State Circuits*, vol. 46, no. 12, pp. 2988–3004, Dec. 2011.
[16] A. Arbabian, S. Callender, S. Kang, B. Afshar, J.-C. Chien, and A. M. Niknejad, "A 90 GHz hybrid switching pulsed-transmitter for medical imaging," *IEEE J. Solid-State Circuits*, vol. 45, no. 12, pp. 2667–2681, Dec. 2010.
[17] H. Riel, L.-E. Wernersson, M. Hong, and J. A. del Alamo, "III-V compound semiconductor transistors—From planar to nanowire structures," *MRS Bull.*, vol. 39, no. 8, pp. 668–677, Aug. 2014.
[18] H. Kanaya, H. Shibayama, S. Suzuki, and M. Asada, "Fundamental oscillation up to 1.31 THz in thin-well resonant tunneling diodes," in *Proc. Int. Conf. Indium Phosph. Rel. Mater. (IPRM)*, Aug. 2012, pp. 106–109.
[19] N. Su, R. Rajavel, P. Deelman, J. N. Schulman, and P. Fay, "Sb-heterostructure millimeter-wave detectors with reduced capacitance and noise equivalent power," *IEEE Electron Device Lett.*, vol. 29, no. 6, pp. 536–539, Jun. 2008.
[20] M. Ärlelid, M. Egard, L. Ohlsson, E. Lind, and L.-E. Wernersson, "Impulse-based 4 Gbit/s radio link at 60 GHz," *Electron. Lett.*, vol. 47, no. 7, pp. 467–468, Mar. 2011.
[21] L. Ohlsson, T. Bryllert, D. Sjöberg, and L.-E. Wernersson, "Monolithically-integrated millimetre-wave wavelet transmitter with on-chip antenna," *IEEE Microw. Wireless Compon. Lett.*, vol. 24, no. 9, pp. 625–627, Sep. 2014.
[22] H.-J. Song and T. Nagatsuma, "Present and future of terahertz communications," *IEEE Trans. Terahertz Sci. Technol.*, vol. 1, no. 1, pp. 256–263, Sep. 2011.
[23] E. Juntunen *et al.*, "A 60-GHz 38-pJ/bit 3.5-Gb/s 90-nm CMOS OOK digital radio," *IEEE Trans. Microw. Theory Techn.*, vol. 58, no. 2, pp. 348–355, Feb. 2010.
[24] J. Lee, Y. Chen, and Y. Huang, "A low-power low-cost fully-integrated 60-GHz transceiver system with OOK modulation and on-board antenna assembly," *IEEE J. Solid-State Circuits*, vol. 45, no. 2, pp. 264–275, Feb. 2010.
[25] A. Siligaris *et al.*, "A low power 60-GHz 2.2-Gbps UWB transceiver with integrated antennas for short range communications," in *Proc. IEEE Radio Freq. Integr. Circuits Symp. (RFIC)*, Jun. 2013, pp. 297–300.
[26] M. Fujishima, M. Motoyoshi, K. Katayama, K. Takano, N. Ono, and R. Fujimoto, "98 mW 10 Gbps wireless transceiver chipset with D-band CMOS circuits," *IEEE J. Solid-State Circuits*, vol. 48, no. 10, pp. 2273–2284, Oct. 2013.
[27] A. Tomkins, R. A. Aroca, T. Yamamoto, S. T. Nicolson, Y. Doi, and S. P. Voinigescu, "A zero-IF 60 GHz 65 nm CMOS transceiver with direct BPSK modulation demonstrating up to 6 Gb/s data rates over a 2 m wireless link," *IEEE J. Solid-State Circuits*, vol. 44, no. 8, pp. 2085–2099, Aug. 2009.
[28] C. Marcu *et al.*, "A 90 nm CMOS low-power 60 GHz transceiver with integrated baseband circuitry," *IEEE J. Solid-State Circuits*, vol. 44, no. 12, pp. 3434–3447, Dec. 2009.
[29] I. Sarkas *et al.*, "An 18-Gb/s, direct QPSK modulation SiGe BiCMOS transceiver for last mile links in the 70–80 GHz band," *IEEE J. Solid-State Circuits*, vol. 45, no. 10, pp. 1968–1980, Oct. 2010.
[30] S. K. Reynolds *et al.*, "A silicon 60-GHz receiver and transmitter chipset for broadband communications," *IEEE J. Solid-State Circuits*, vol. 41, no. 12, pp. 2820–2831, Dec. 2006.
[31] A. Siligaris *et al.*, "A 65 nm CMOS fully integrated transceiver module for 60 GHz wireless HD applications," in *Proc. IEEE Int. Conf. Solid-State Circuits Tech. Dig. Papers (ISSCC)*, Feb. 2011, pp. 162–163.

LARS OHLSSON received the M.Sc. degree in engineering nanoscience from Lund University, Lund, Sweden, in 2010, where he is currently pursuing Ph.D. degree with the Department of Electrical and Information Technology.

He performs circuit design and develops technology for integrated antennas and millimeter-wave pulse generators. He further explores pulse-based communication and time-domain characterization. His research interests include integrated antennas, pulse generator circuits, device characterization, antenna codesign, and millimeter-wave pulse-based systems.

LARS-ERIK WERNERSSON received the M.Sc. degree in engineering physics and the Ph.D. degree in solid-state physics from Lund University, Lund, Sweden, in 1993 and 1998, respectively.

He has been a Professor of Nanoelectronics with Lund University since 2005, and was a Visiting Associate Professor with the University of Notre Dame, Notre Dame, IN, USA, in 2002 and 2003. His main research interests include design and fabrication of nanowire- and tunneling-based nanoelectronic devices and circuits with applications in low-power electronics and wireless communication. He has authored or co-authored over 120 scientific papers in this area.

Dr. Wernersson has been awarded two individual career grants from the Swedish Foundation for Strategic Research.